Endokrynologia Polska
DOI: 10.5603/EP.a2016.0026
Tom/Volume 67; Numer/Number 2/2016
ISSN 0423–104X

Differentiation of thyroid nodules in multinodular goitre with the application of technical ultrasound advances — initial results

Różnicowanie zmian ogniskowych w wolu guzkowym tarczycy z zastosowaniem nowych technik ultrasonograficznych — doniesienia wstępne

Bartosz Migda[1], Rafał Słapa[1], Jacek Bierca[2], Jadwiga Słowińska-Srzednicka[3], Anna Migda[4], Katarzyna Dobruch-Sobczak[5], Wiesław Jakubowski[1]

[1]Department of Diagnostic Imaging, Second Faculty of Medicine with the English Division and the Physiotherapy Division, Medical University of Warsaw, Poland
[2]Surgery Department, Solec Hospital, Warsaw, Poland
[3]Department of Endocrinology, Centre for Postgraduate Medical Education, Warsaw, Poland
[4]First Department of Internal Diseases, Bielanski Hospital, Warsaw, Poland
[5]Institute of Fundamental Technological Research, Polish Academy of Sciences, Warsaw, Poland

Abstract

Introduction: To evaluate the relative value of technical ultrasound advances in differentiation of thyroid nodules in multinodular goitre.
Material and methods: The study included patients with multinodular goitre, who were referred for thyroidectomy. Ultrasound evaluation of suspicious nodules was performed with: improved B-mode (spatial compound imaging and differential tissue harmonics), dedicated mapping of microcalcifications, mapping of the nodule vessels, and strain elastography evaluated qualitatively and semi quantitatively.
Results: A total of 163 nodules in 124 patients with multinodular goitre were evaluated (147 benign and 16 cancers). Improved B-mode imaging was: 76.76% sensitive and 62.5% specific with AUC 0.740. Differentiating B-mode features were: shape — taller than wide OR 15.8, markedly hypoechoic OR 14.7, absence of cystic areas OR 6.6, absence of halo OR 5.0, and blurred/microlobulated margins OR 3.7. Addition of MicroPure imaging was 80.28% sensitive and 68.75% specific with AUC 0.771. MicroPure alone, power Doppler, and strain elastography were not statistically significant.
Conclusions: Among singular modes of ultrasound imaging, only improved B-mode imaging proved to have a significant role in differentiation of thyroid nodules in multinodular goitre. Additional gain was seen with the addition to B-mode of the mapping of microcalcifications with MicroPure imaging. Power Doppler and strain elastography did not prove to be useful techniques in multinodular goitre. **(Endokrynol Pol 2016; 67 (2): 157–165)**

Key words: *thyroid; goitre nodular; ultrasonography; elasticity imaging techniques; ultrasonography Doppler*

Streszczenie

Wstęp: Celem pracy była ocena względnej wartości nowych technik ultrasonograficznych w różnicowaniu zmian ogniskowych w wolu guzkowym.
Materiał i metody: Grupa badana obejmowała chorych z wolem guzkowym przed planowaną tyreoidektomią. Protokół badania ultrasonograficznego obejmował: B-mode z użyciem obrazowania złożonego przestrzennie oraz tkankowego obrazowania harmonicznego, mapowanie mikrozwapnień, mapowanie naczyń oraz elastogafię odkształceń względnych (ocena jakościowa i półilościowa).
Wyniki: Oceniono w sumie 163 zmiany ogniskowe u 124 pacjentów (147 zmian łagodnych i 16 raków). Czułość, swoistość i AUC dla B-mode z użyciem obrazowania złożonego przestrzennie oraz tkankowego obrazowania harmonicznego wynosiły odpowiednio 76,76%, 62,5% oraz 0,740. Wśród ocenionych cech obrazowania B-mode różnicującymi okazały się być: kształt (zmian wyższa niż szersza OR 15,8), bardzo niska echogeniczność OR 14,7, brak zwyrodnień płynowych OR 6,6, brak otoczki halo OR 5,0 oraz zatarte/zrazikowe granice OR 3,7. Wzbogacenie obrazowania B-mode o obrazowanie Micropure zwiększyło czułość 80,28% i swoistość 68,75%, AUC 0,771.
Obrazowanie Micropure, Power Doppler oraz elastografia odkształceń względnych jako samodzielne metody okazały się być nie istotne statystycznie w różnicowaniu zmian łagodnych i złośliwych.
Wnioski: Wśród pojedynczych metod ultrasonograficznych jedynie wzbogacone obrazowanie B-mode okazało się być istotne w różnicowaniu zmian ogniskowych w wolu guzkowym tarczycy. Dodatkowym zyskiem było dołączenie do oceny B-mode mapowanie mikrozwapnień z zastosowaniem techniki Micropure. Power Doppler oraz elastografia odkształceń względnych okazały się być nieprzydatne w różnicowaniu zmian ogniskowych w wolu guzkowym tarczycy. **(Endokrynol Pol 2016; 67 (2): 157–165)**

Słowa kluczowe: *tarczyca; wole guzkowe; ultrasonografia; elastografia; ultrasonografia Doppler*

This paper was supported by Grant N N402 476437 (2009-2012) from the Ministry of Science and Higher Education of Poland.

Bartosz Migda M.D., Department of Diagnostic Imaging Medical University of Warsaw, Kondratowicza St. 8, 03–242 Warsaw, Poland, phone: +48 22 326 58 10, fax: +48 22 326 59 91, e-mail: bartoszmigda@gmail.com

Introduction

Ultrasound enables visualisation of thyroid nodules in a high percentage of the population, reaching 30–70% [1]. Nodular goitres are clinically recognisable enlargements of the thyroid gland characterised by excessive growth and structural and/or functional transformation of one or several areas within the normal thyroid tissue[2]. Most thyroid incidentalomas are benign; however, some papers report that the percentage of cancer in these group of patients is high, reaching 17%. This implies the necessity of ultrasound and biopsy evaluation in these groups of patients[3]. Determination of thyroid nodules for biopsy is especially important in nodular goitre patients. On ultrasound examinations nodular goitre is frequently diagnosed, especially in the group of older people and in areas of iodine deficiency. The prevalence of thyroid cancer in patients with a multinodular goitre is not firmly established, with reported rates in the literature ranging between 3 and 35%, and there is no difference whether the gland contains a single nodule or multiple nodules [4].

In recent years many new ultrasound applications from B-mode optimisation, flow imaging, microcalcifications mapping, and elastography have been implemented to clinical ultrasound scanners.

The aim of our study was to evaluate the relative value of technical ultrasound advances in differentiation of thyroid nodules in multinodular goitre.

Material and methods

The study was approved by the Local Bioethical Committee. Each patient gave informed consent before enrolment. The study included examinations performed between January 2009 and April 2014. The study involved patients with multinodular goitre, who were scheduled for thyroidectomy (because of: compression symptoms, cosmetic defect, diagnosis or suspicion of malignancy, and hormonal imbalance).

Selection of the nodules for the analysis with advanced ultrasound techniques (enhanced B-mode, MicroPure, Power Doppler and Strain Elastography) included any combination of the following thyroid nodule ultrasound suspicious features: shape taller than wide, low echogenicity, irregular margins, high echogenicity foci, central or mixed vascularisation, and dominant nodule by ultrasound features in the ultrasound presentation of nodular goiter [5, 6].

The examination was performed with a Toshiba (Japan) Aplio XG scanner, with high frequency 7–18 MHz linear transducer with field of view width of 38 mm. The ultrasound examinations were performed with factory settings optimised for thyroid imaging including trapezoid field of view for all modes except for elastography.

The protocol included the following methods:

— B-mode with simultaneous application of new image improvement techniques such as spatial compound imaging and differential tissue harmonics (Fig. 1A left);
— Mapping of the microcalcifications — MicroPure (Fig. 1A right);
— Power Doppler (Fig. 1B);
— Strain Elastography – qualitative and semiquantitative (Elasto-Q) (Fig. 1C, D).

Strain elastography images included part of the thyroid parenchyma and possibly the whole nodule. However, in order to maximise the number of suspicious nodules to be evaluated we also included the nodules that were visualised partially. Cystic degenerations and macrocalcifications were not exclusion criteria for further elastographic analysis of the nodules. However, the semiquantitative strain measurements included only the solid parts without macrocalcifications. The representative images were stored in digital form.

Assessed features included: B-mode — echogenicity, margins, halo, microcalcifications, macrocalcifications, eggshell calcification, comet tail artefact, cystic areas in the nodule, shape of the nodule taller than wide (axial plane), mean lesion diameter, and lesion volume.

MicroPure imaging (punctate high echogenicity foci on blue background), Power Doppler I — Lack of vessels in the nodule; II — dominant peripheral vessels in the nodule, III — dominant central vessels in the nodule, IV — mixed vessels structure, both peripheral and central,

Strain Elastography:

— Qualitative assessment — Elasticity Index [7];
— Semiquantitative assessment — Strain Ratio evaluation.

Statistical analysis

Statistical analysis was performed with STATISTICA 10 (StatSoft Inc.) and RapidMiner. W Shapiro-Wilk test, U Mann-Whitney test Chi2 test were performed. AUC ≥ 0.7 and $p < 0.05$ were considered significant.

Results

The research group consisted of 124 patients with multinodular goitre, who were referred for thyroidectomy (110 women and 14 men). In total 163 nodules were evaluated (147 benign and 16 cancers).

The malignant lesions were 16 papillary cancers (including 4 follicular variant and 1 oxyphilic variant).

21 patients had a coexisting autoimmune disease (19 Hashimoto disease, 2 Graves-Basedow disease), that represented 17% of all patients.

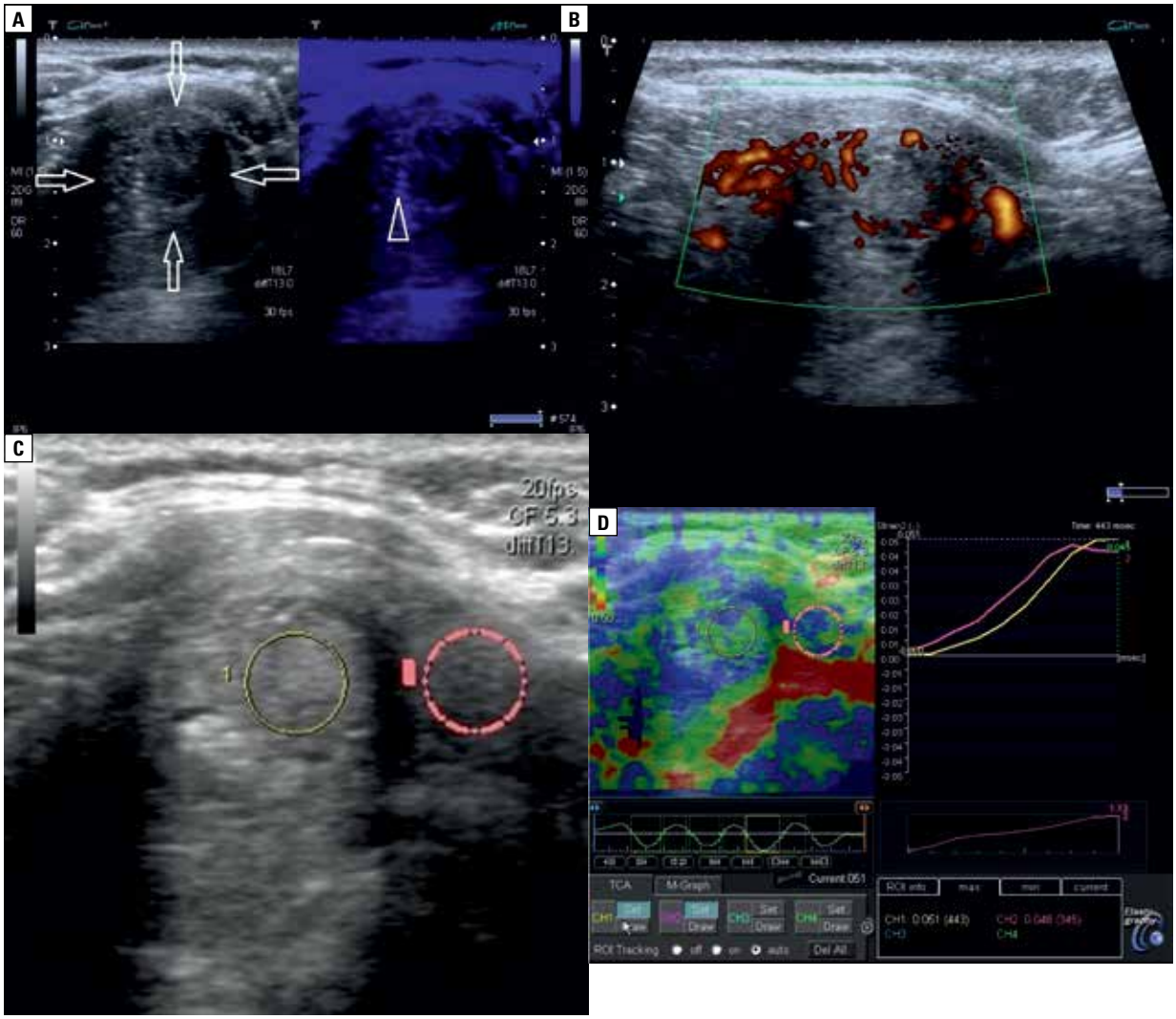

Figure 1. *Papillary cancer in right lobe of thyroid in patient with multinodular goitre and Hashimoto disease. Size of the lesion:16 × 13 × 15 mm.* **A.** *On B-mode presentation (left) lesion is marked with arrows. On MicroPure imaging (right) arrow head is pointing out the microcalcifications. Microcalcifications are visible on both B-mode and MicroPure imaging;* **B**. *On Power Doppler the nodule presented the mixed vascularisation;* **C**. *B-mode with marked ROI in the nodule (yellow) avoiding calcifications and ROI at the same depth in the thyroid tissue (pink) with corresponding elastography image;* **D**. *Elasticity Index 1. Strain Ratio 0.94.*

Rycina 1. *Rak brodawkowaty prawego płata tarczycy u pacjenta z wolem guzkowym w przebiegu choroby Hashimoto. Wymiar zmiany: 16 × 13 × 15 mm.* **A.** *Prezentacja B-mode (strona lewa) zmiana zaznaczona strzałkami. Obrazowanie MicroPure (strona prawa) grotem strzałki zaznaczono mikrozwapnienia. Mikrozwapnienia są widoczne zarówno w obrazowaniu B-mode, jak i MicroPure.* **B.** *W obrazowaniu Power Doppler zmiana wykazuje mieszany typ unaczynienia.* **C.** *W prezentacji B-mode zaznaczono ROI w guzku (kolor żółty), unikając zwapnień, oraz ROI na tej samej głębokości w referencyjnej tkance tarczycowej (kolor różowy).*

B-mode

B-mode ultrasound characteristics of the thyroid nodules and B-mode features that differentiate benign and malignant lesions are presented in Table I and II.

Mean diameters and volume of nodules were bigger for benign lesions than malignant ones and were 23.9 mm *vs.* 17.5 mm and 11.5 cm^3 *vs.* 8.4 cm^3 respectively. These differences where statistically significant (diameter p = 0.0001, volume p = 0.0233).

Micropure imaging

Presence of microcalcifications on B-mode did not prove to be a differential factor between malignant and benign nodules, p = 0.0840. Additional application of specialized software, Micropure imaging, did not improve differentiation (p = 0.1860), increased sensitivity (75.0% *vs.* 68.8%) but decreased specificity (47.7% *vs.* 54.4%).

Table I. *B-mode ultrasound characteristics of the thyroid nodules (significant differentiating features marked with bold characters)*

Tabela I. *Cechy obrazowania B-mode zmian ogniskowych (istotne statystycznie cechy wytłuszczono)*

B-mode features		Benign	Malignant	p
		N (%)	N (%)	
Echogenicity	**Markedly hypoechoic**	**15 (10.2)**	**10 (62.5)**	**0.0000****
	Hypoechoic	39 (26.5)	2 (12.5)	0.3470**
	Markedly hypoechoic and hypoechoic	**54 (36.7)**	**12 (75.0)**	**0.003***
	Isoechoic	39 (26.5)	1 (6.3)	0.1473**
	Hyperechoic	4 (2.8)	0 (0.0)	0.8733**
	Mixed echogenicity	50 (34.0)	3 (18.7)	0.3216
Margins	**Sharp**	**116 (78.9)**	**8 (50.0)**	**0.0104****
	Blurred/microlobulated	**31 (21.1)**	**8 (50.0)**	
Halo	**Absent**	**56 (38.1)**	**12 (75.0)**	**0.0036***
	Present	**91 (61.9)**	**4 (25.0)**	
Macrocalcifications	Absent	99 (67.3)	13 (81.2)	0.3487*
	Present	48 (32.7)	3 (18.8)	
Microcalcifications	Absent	78 (53.1)	5 (31.3)	0.084*
	Present	69 (46.9)	11 (68.7)	
Comet tail artefact	Absent	137 (93.2)	15 (93.7)	0.6891**
	Present	10 (6.8)	1 (6.3)	
Eggshell calcifications	Absent	144 (98.0)	16 (100)	0.7046**
	Present	3 (2.0)	0 (0.0)	
Cystic areas in the nodule	**Absent**	**46 (31.3)**	**12 (75.0)**	**0.0005***
	Present	**101 (68.7)**	**4 (25.0)**	
Taller than wide	**Absent**	**129 (87.8)**	**5 (31.3)**	**0.0458****
	Present	**18 (12.2)**	**11 (68.7)**	

*p value for Chi2 test; **p value for Chi2 test with Yates correction; markedly hypoechoic: echogenicity of nodule lower or equal to strap muscles

Table II. *B-mode features that differentiate benign and malignant lesions*

Tabela II. *Cechy obrazowania B-mode różnicujące zmiany łagodne i złośliwe*

B-mode	Malignant %	Benign %	P	OR	CI	Sensitivity %	Specificity %
Shape taller than wide	68.7	12.2	0.0458**	15.8	4.9–50.6	68.7	87.8
Markedly hypoechoic	62.5	10.2	0.0000**	14.7	4.7–46.1	62.5	89.8
Absence of cystic areas	75.0	31.3	0.0005*	6.6	2.0–21.5	75.0	68.7
Markedly hypoechoic and hypoechoic	75.0	36.7	0.0030**	5.2	1.6–16.8	75.0	63.2
Absence of halo	75.0	38.1	0.0036*	5.0	1.5–15.8	75.0	61.9
Blurred/microlobulated margins	50.0	21.1	0.0104**	3.7	1.3–10.8	50.0	78.9

*p value for Chi2 statistics; **p value for Chi2 statistics with Yates correction; OR — odds ratio; CI — confidence interval

Power Doppler

Four grade scale was adopted for evaluation of thyroid nodules with Power Doppler.

Most of the malignant lesions were vascularized (81.3%), with most frequent peripheral vascularization (37.5%) and mixed vascularization (31.3%).

Most of the benign lesions were also vascularized (88.4%), with peripheral vascularization in 40.8% and mixed vascularization in 36.7%.

Among assessed vascular patterns none of them was statistical significant $p > 0.05$.

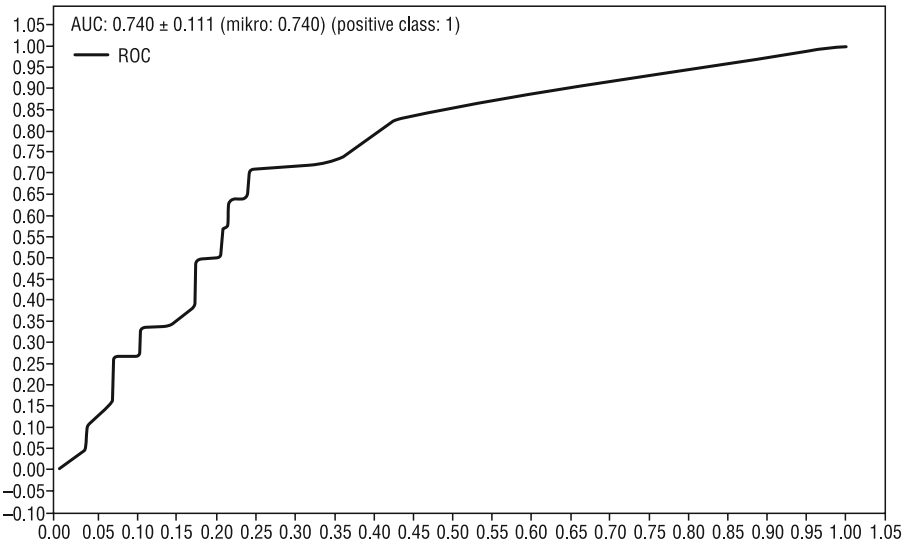

Figure 2. *ROC graph for improved B-mode imaging*
Rycina 2. *ROC dla wzbogaconego obrazowania B-mode*

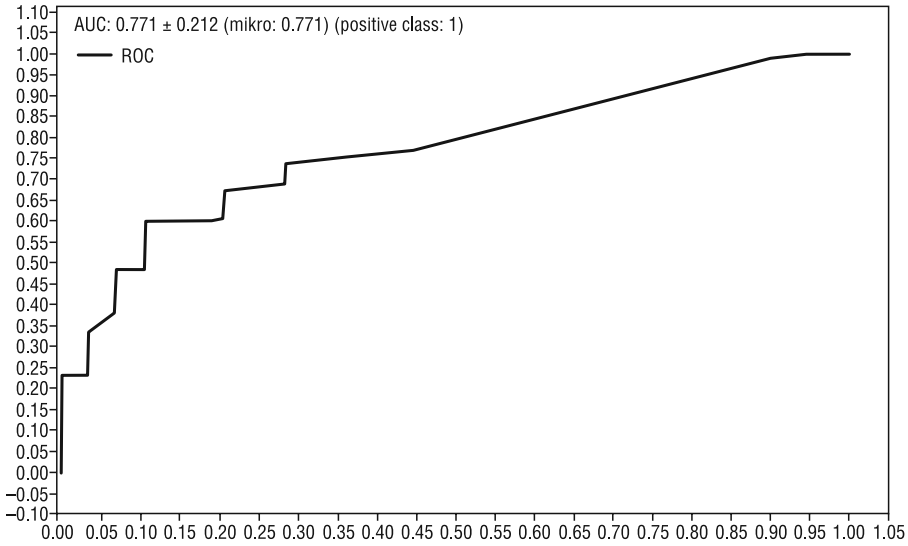

Figure 3. *ROC graph for improved B-mode imaging and MicroPure imaging*
Rycina 3. *ROC dla wzbogaconego obrazowania B-mode i obrazowania Micropure*

Strain Elastography

The whole nodule with part of surrounding thyroid parenchyma was visible and evaluated with elastography in 59.3%. The remaining 40.7% nodules were so large that only part of the crossection of the nodule was possible to be visualized and evaluate with margin of thyroid parenchyma on one elastography image.

Differentiation with Elasticity Index was statistically insignificant $p > 0.05$, OR range 0.5–2.0.

Semi-quantitative analysis with Strain Ratio did not revealed any differences in malignant and benign lesions, $p = 0.0741$. ROC analysis was insignificant, AUC = 0.404.

Data mining

Statistical analysis revealed that among the singular advanced ultrasound methods, improved B-mode imaging proved to be the best one (sensitivity 76.76%, specificity 62.5%, accuracy 75.36%, AUC 0.740) (Fig. 2).

Among single methods and their combinations, model B-mode and MicroPure imaging presented the best discriminatory power, AUC = 0.771, with sensitivity 80.28%, specificity 68.75%, and accuracy 79.17% (Fig. 3).

Model B-mode and Strain Elastography presented lower discriminatory power than that mentioned above, AUC = 0.712, with sensitivity 78.17%, specificity 50%, and accuracy 75.24% (Fig. 4).

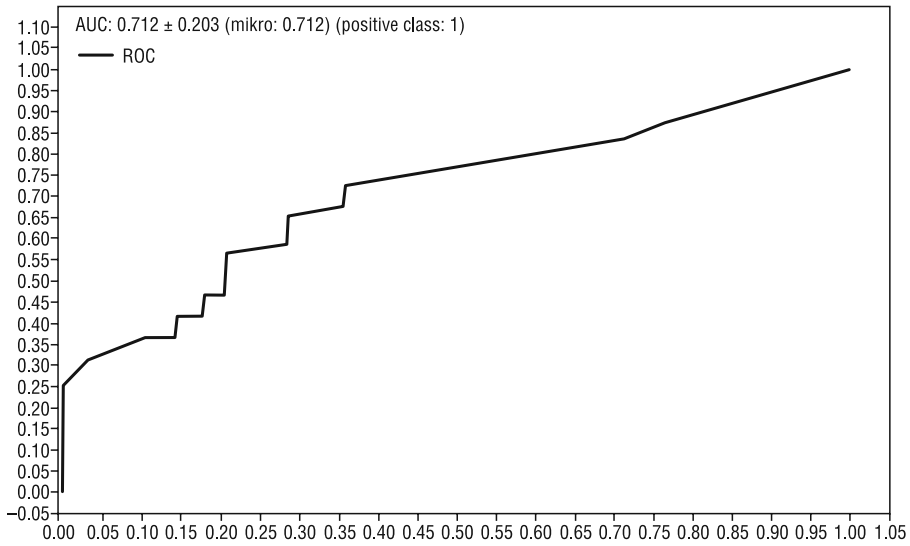

Figure 4. *ROC graph for improved B-mode imaging and strain elastography*
Rycina 4. *ROC dla wzbogaconego obrazowania B-mode i elastografii odkształceń względnych*

Table III. ***Diagnostic methods and their combinations***
Tabela III. ***Porównanie nowych technik ultrasonograficznych i ich kombinacji***

Diagnostic method	Sensitivity (%)	Specificity (%)	Accuracy (%)	AUC
B-mode	**76.76**	**62.50**	**75.36**	**0.740**
MicroPure	75.00	47.60	50.00	0.493
Power Doppler	83.80	12.50	16.67	0.468
Strain Elastography	85.21	25.00	23.33	0.536
B-mode + MicroPure	**80.28**	**68.75**	**79.17**	**0.771**
B-mode + Power Doppler	74.65	18.75	18.33	0.578
B-mode + Strain Elastography	**78.17**	**50.00**	**75.24**	**0.712**
MicroPure + Power Doppler	70.42	37.50	40.00	0.528
Micropure + Strain Elastography	88.03	31.25	25.00	0.623
Power Doppler + Strain Elastography	83.80	25.00	21.67	0.500
B-mode + MicroPure + Power Doppler	77.46	56.25	23.45	0.643
B-mode + MicroPure + Strain Elastography	70.42	43.75	45.00	0.598
B-mode + Power Doppler + Strain Elastography	75.35	20.28	17.95	0.687
MicroPure + Power Doppler + Strain Elastography	76.06	25.00	33.33	0.604
B-mode + Micropure + Power Doppler + Strain Elastography	75.87	26.03	23.52	0.693

An important threshold for AUC not less than 0.7 — marked with bold character

Other combinations presented AUC values under 0.7 (Table III).

Discussion

In recent years many ultrasound technical advances have been evaluated in regard to thyroid pathology. These include techniques that improve quality of B-mode images, like harmonic imaging [8] and compound spatial imaging [9], or altered the presentation of ultrasound data, like panoramic or trapezoid field of view ultrasound , 3D ultrasound [10], or MicroPure imaging [11]. The vascularisation of the nodules was assessed with Colour or Power Doppler [12] or by using contrast agents [13]. In our study, among singular modes of ultrasound imaging, only improved B-mode imaging proved to have a significant role in differentiation of thyroid nodules. Additional gain was seen by the ad-

dition to B-mode evaluation of high echogenicity foci with MicroPure imaging.

The statistically significant B-mode ultrasound features that suggested malignancy included: shape — taller than wide, markedly hypoechoic, absence of cystic areas, absence of halo, and blurred/microlobulated margins.

In this study the markedly hypoechoic criterion was defined differently than in previous studies [6] because then we included to this group the lesions with echogenicity equal to or lower than the echogenicity of strap muscles. However, the contrast on B-mode imaging was influenced by technical advancements such as combined compound imaging and tissue harmonic imaging. These two techniques also influence the presentation of high echogenicity foci, enhancing their visibility but conversely influencing their posterior artefacts (comet tail artefacts or acoustic shadow). We cannot be sure about the precise influence of joint application of both techniques on the presentation of posterior artefacts on the image because the spatial compound imaging reduces the artefacts and tissue harmonic imaging enhances them [14].

The cancers in our series included papillary carcinomas only. In the literature these present microcalcifications with high specificity (85.8–95%), although with poor sensitivity in the range 25–40%, but in some series in as many as 90% [15]. However, in our study microcalcifications proved to be an insignificant feature of malignancy with higher sensitivity (68.8%) but with decreased specificity (54.4%) in contrast to literature data. This may be partly because inspissated colloid in benign nodules may present as microcalcifications without visible comet tail artefacts. This finding seems to be more typical for nodules in multinodular goitre than in single thyroid nodules. Furthermore, the presence of the ring-down artefact does not necessarily preclude contemplating biopsy; microcalcifications and colloid may coexist in the same nodule [16]. The impossibility of distinguishing between microcalcifications and inspissated colloid could also influence the dedicated microcalcifications imaging with MicroPure technique. MicroPure as a sole technique did not prove to be statistically significant enough to differentiate thyroid nodules, even with increasing sensitivity to 75.0% and decreasing specificity to 47.6%. However, its combination with B-mode imaging improved the discriminatory power of B-mode imaging.

Spatial compound imaging and harmonic imaging reduce speckles and improve margin delineation. In our study blurred/microlobulated margins proved to be a single predictor of malignancy, with sensitivity of 50% and specificity of 78.9%. Improved detection of blurred margins may indicate malignancy, but it may also be a marker of aggressive behaviour of papillary thyroid carcinoma [6, 17].

The new and most specific discriminatory power features were described by Kim et al., which are parallel to breast cancer features and include: shape taller than wide and markedly hypoechogenic — in our study this presented the best discriminatory power, with sensitivity 68.7% and 62.5% (that was much higher than in the Kim study at 32.7% and 26.5%, respectively) and specificity 87.8% and 89.8% (similar to the Kim study), respectively. This could be partly attributed to the application of spatial compound and tissue harmonic imaging in our study.

Despite initial expectations regarding the discriminatory power of Doppler techniques, the newest option the Power Doppler in our study did not prove to be useful, as presented recently in the literature [12].

Strain elastography, which was used in our study, assesses the elastic properties of tissues by analysing tissue strain, i.e. tissue deformation parallel to direction of the exploratory force. Deformation in our study was induced by slight compression with probe by the ultrasonologist. For the classification of the nodule stiffness qualitatively, the most widely recently used 4 grade Asteria scale was applied [7]. The second, semiquantitiave approach included the ratio of thyroid parenchyma strain to the nodule one. Some cases of multinodular goitre were disqualified from our study because of lack of ultrasound-visible thyroid parenchyma, which is an unavoidable disadvantage in characterising some cases of this disease. A characteristic feature of many cases of multinodular goitres is large diameter of the nodules, which resulted in partial visualisation of the nodule together with portion of thyroid parenchyma in our material — in 40.7% of nodules. According to some opinions, evaluated nodules should be visualised with elastography image as a whole [14]. Even in this approach the nodule is examined partially in the plane chosen by the operator. To examine the possibility of characterisation of ultrasonographically suspicious nodules in multinodular goitre by elastography, we decided to include into the analysis the nodules that could be only partially visualised with surrounding thyroid parenchyma, which is necessary for proper evaluation of the nodule strain.

Both qualitative and semiquantitative approaches in the case of nodular goitre patients proved not to be useful for differentiation of thyroid nodules, $p>0.05$. Joint analysis of B-mode and strain elastography (qualitative and semiquantitative approach) did not exceed the discriminatory power of B-mode assessment (AUC 0.712 *vs.* 0.740). This is consistent with the literature [18–20]. It may be attributable to the location and neighbourhood of the thyroid on the neck, with location of the lateral

lobes in the groove between sternocleidomastoid muscle and trachea, resulting in the oblique movements of the thyroid gland and nodules upon vertical compression with the probe by the operator. These movements with a lateral component may introduce error to the measurement of the strain in free-hand elastography. This probably cannot be overcome even by carotid pulsation elastography,which did not incorporate the compression by the operator. In this technique carotid pulsation compression also involves oblique planes and is unpredictable. Moreover, carotid pulsation elastography cannot be applied for the nodules located far from carotid arteries as in thyroid isthmus [21].

Similarly to shadowing, reverb, and clutter artefacts that can be present in B-mode images, elasticity images are susceptible to their own artefacts, which clinicians must be trained to accommodate during their interpretation. Tissue compression can lead to strain concentration artefacts around structures,which can lead to distortions in the strain fields [22]. This may be especially significant in the case of multinodular goitre, where the elasticity of one nodule may be influenced by the elasticity of the surrounding nodules.

The poor performance of elastography in our study may be partly attributed to the features of multinodular goitre. This could be overcome by shear-wave elastography, which evaluates the stiffness in the nodules in absolute values as kPa or m/s. It does not necessarily require the reference thyroid parenchyma tissue to be present and may evaluate in real time the stiffness of the whole nodule even if it is large in several imaging planes. It may enable measurement of the E plane by plane, resulting in evaluation of this value for the entire nodule. However, even in this technique, cut off values optimised for diagnosis of malignancy, in studies using identical SWE technology, range between 42.1 kPa and 65 kPa and corresponding diagnostic performances range between 52.9% sensitivity, 77.8% specificity, and 85.2% sensitivity, 93.9% specificity [23, 24]. In evaluation of multinodular goitre this problem of different thresholds could possibly be solved with approach of Wolinski et al. [25], who referred the hardest nodules in the multinodular goitre for fine-needle aspiration biopsy (FNAB), irrespectively of the already published cutoff values.

The limitations of our study include: retrospective character, small number of cancer cases, only papillary cancer malignancies, and the width of the probe.

Conclusions

Among singular modes of ultrasound imaging, only improved B-mode imaging proved to play a significant role in the differentiation of thyroid nodules in multinodular goitre. Additional gain was made by the addition to B-mode of the mapping of microcalcifications with MicroPure imaging. Power Doppler and strain elastography did not prove to be useful techniques in multinodular goitre.

References

1. Ross DS. Editorial: Non-palpable thyroid nodules-managing an epidemic. J Clin Endocrinol Metab 2002; 87: 1938–1940. doi: 10.1210/jc.87.5.1938
2. Hegedus L, Bonnema SJ, Bennedbaek FN. Management of simple nodular goiter: current status and future perspectives. Endocrine Reviews 2003; 24: 102–132. doi: 10.1210/er.2002-0016
3. Liebeskind A, Sikora AG, Komisar A et al. Rates of malignancy in incidentally discovered thyroid nodules evaluated with sonography and fine-needle aspiration. J Ultrasound Med 2005; 24: 629–634.
4. Gandolfi PP, Frisina A, Raffa M et al. The incidence of thyroid carcinoma in multinodular goiter: retrospective analysis. Acta bio-medica: Atenei Parmensis 2004; 75: 114–117.
5. Chan BK, Desser TS, McDougall IR et al. Common and uncommon sonographic features of papillary thyroid carcinoma. J Ultrasound Med 2003; 22: 1083–1090.
6. Kim EK, Park CS, Chung WY et al. New sonographic criteria for recommending fine-needle aspiration biopsy of nonpalpable solid nodules of the thyroid. AJR Am J Roentgenol 2002; 178: 687–691. doi: 10.2214/ajr.178.3.1780687
7. Asteria C, Giovanardi A, Pizzocaro A et al. US-elastography in the differential diagnosis of benign and malignant thyroid nodules. Thyroid 2008; 18: 523–531. doi: 10.1089/thy.2007.0323
8. Szopinski KT, Wysocki M, Pajk AM et al. Tissue harmonic imaging of thyroid nodules: initial experience. J Ultrasound Med 2003; 22: 5–12.
9. Bartolotta TV, Midiri M, Runza G et al. Incidentally discovered thyroid nodules: incidence, and greyscale and colour Doppler pattern in an adult population screened by real-time compound spatial sonography. Radiol Med 2006; 111: 989–998. doi: 10.1007/s11547-006-0097-1
10. Slapa RZ, Jakubowski WS, Slowinska-Srzednicka J et al. Advantages and disadvantages of 3D ultrasound of thyroid nodules including thin slice volume rendering. Thyroid Res 2011; 4: 1. doi: 10.1186/1756-6614-4-1
11. Ciledag N, Arda K, Aribas BK et al. The utility of ultrasound elastography and MicroPure imaging in the differentiation of benign and malignant thyroid nodules. AJR Am J Roentgenol 2012; 198: W244–249. doi: 10.2214/AJR.11.6763
12. Moon HJ, Kwak JY, Kim MJ et al. Can vascularity at power Doppler US help predict thyroid malignancy? Radiology 2010; 255: 260–269. doi: 10.1148/radiol.09091284
13. Nemec U, Nemec SF, Novotny C et al. Quantitative evaluation of contrast-enhanced ultrasound after intravenous administration of a microbubble contrast agent for differentiation of benign and malignant thyroid nodules: assessment of diagnostic accuracy. Eur Radiol 2012; 22: 1357–1365. doi: 10.1007/s00330-012-2385-6
14. McQueen AS, Bhatia KS. Thyroid nodule ultrasound: technical advances and future horizons. Insights into imaging 2015. doi: 10.1007/s13244-015-0398-9
15. Sofferman RA, Ahuja A.T. Ultrasound of the thyroid and parathyroid glands. Springer, 2012.
16. Coquia SF, Chu LC, Hamper UM. The role of sonography in thyroid cancer. Radiologic clinics of North America 2014; 52: 1283–1294. doi: 10.1016/j.rcl.2014.07.007
17. Ito Y, Kobayashi K, Tomoda C et al. Ill-defined edge on ultrasonographic examination can be a marker of aggressive characteristic of papillary thyroid microcarcinoma. World J Surg 2005; 29: 1007–1011; discussion 11-2. doi: 10.1007/s00268-005-7834-9
18. Kagoya R, Monobe H, Tojima H. Utility of elastography for differential diagnosis of benign and malignant thyroid nodules. Otolaryngol Head Neck Surg 2010; 143: 230–234. doi: 10.1016/j.otohns.2010.04.006
19. Lippolis PV, Tognini S, Materazzi G et al. Is elastography actually useful in the presurgical selection of thyroid nodules with indeterminate cytology? J Clin Endocrinol Metab 2011; 96: E1826–1830. doi: 10.1210/jc.2011-1021
20. Moon HJ, Sung JM, Kim EK et al. Diagnostic performance of gray-scale US and elastography in solid thyroid nodules. Radiology 2012; 262: 1002–1013. doi: 10.1148/radiol.11110839

21. Dighe M, Bae U, Richardson ML et al. Differential diagnosis of thyroid nodules with US elastography using carotid artery pulsation. Radiology 2008; 248: 662–669. doi: 10.1148/radiol.2482071758
22. Palmeri ML, Nightingale KR. What challenges must be overcome before ultrasound elasticity imaging is ready for the clinic? Imaging in medicine 2011; 3: 433–444. doi: 10.2217/iim.11.41
23. Bhatia KS, Tong CS, Cho CC et al. Shear wave elastography of thyroid nodules in routine clinical practice: preliminary observations and utility for detecting malignancy. Eur Radiol 2012; 22: 2397–2406. doi: 10.1007/s00330-012-2495-1
24. Sebag F, Vaillant-Lombard J, Berbis J et al. Shear wave elastography: a new ultrasound imaging mode for the differential diagnosis of benign and malignant thyroid nodules. J Clin Endocrinol Metab 2010; 95: 5281–5288. doi: 10.1210/jc.2010-0766
25. Wolinski K, Szczepanek-Parulska E, Stangierski A et al. How to select nodules for fine-needle aspiration biopsy in multinodular goitre. Role of conventional ultrasonography and shear wave elastography — a preliminary study. Endokrynol Pol 2014; 65: 114–118. doi: 10.5603/EP.2014.0016.